CHAPTER 15

ASTER and DEM change assessment of glaciers near Hoodoo Mountain, British Columbia, Canada

Jeffrey Kargel, Gregory Leonard, Roger Wheate, and Benjamin Edwards

ABSTRACT

Hoodoo Mountain ice cap, Hoodoo Glacier, and Twin Glacier are located about 250 km southeast of Juneau, Alaska, in the Coast Mountains (near 56.8°N, 131.3°W, northwestern British Columbia). Several outlet valley glaciers flow towards the south from an ice cap centered approximately 16 km northeast of Hoodoo Mountain; some glaciers are relatively clean ice, while others are heavily debris covered. Hoodoo and Twin glaciers have a Pleistocene and Early Holocene record of interaction with a trachyte volcano, Hoodoo Mountain (which is still ice capped), though they have retreated far enough that future eruptions are unlikely to produce direct lava–ice interactions from anything other than long-lived lava flows. Our analysis shows retreat and accelerating thinning for valley glaciers within this study; this behavior appears to be climatically driven. However, the small ice cap on Hoodoo Mountain seems to be insensitive to climate change; rather, the ice cap's extent is controlled mainly by the shape and elevation of the landform. The overall average mass balance of the combined set of glaciers in the study region was about -840 ± 180 kg m^{-2} yr^{-1} for the period from 1965 to 2005, though different glaciers have specific mass balances ranging from near zero (i.e., in local balance) to $-2{,}400$ kg m^{-2} yr^{-1}. Furthermore, the documented increase in the rate of thinning indicates an increasing magnitude of negative balances over the four decades of the study period. Aside from the Hoodoo Mountain ice cap (which is close to a balance state, except at the very edges on the cliffs, where retreat and thinning have taken place), the prevalent glacier thinning and retreat of the Hoodoo Mountain area is similar to most other maritime parts of the Canadian Cordillera (see Chapter 14 of this book by Wheate et al.). Hoodoo Mountain is a classic flat-topped glaciovolcanic edifice (tuya), and was shaped when ice was much thicker within the massive Cordilleran Ice Sheet. Continuing glacial retreat from the flanks of Hoodoo Mountain offers new possibilities for the study of fresh exposures of materials formed by ice interactions with a rare lava type.

15.1 INTRODUCTION

This chapter offers some novel approaches in data visualization of glacier changes discerned for ice caps and outlet glaciers on and near Hoodoo Mountain, northwestern British Columbia (whose location is given in Fig. 15.1; see also Fig. 14.1). Due to the remoteness of the Hoodoo Mountain area it is most readily studied by satellite remote sensing. Our main objectives are (1) to use digital elevation data obtained over four decades of

Figure 15.1. Image map showing the locations of Hoodoo Mountain, the Andrei Icefield (informal name), and two weather stations (red squares) at Stewart and Dease Lake. Also shown is an ASTER image footprint containing Hoodoo Mountain. The Alaska panhandle/British Columbia border is shown in black, and the British Columbia/Yukon Territory border is in white.

mapping and analysis to assess glacier mass balance, and (2) to use satellite and ground-based repeat imaging to characterize the main geomorphological and process changes that may relate to glacier dynamics and mass balance versus those that are due to interannual, weather cycle, or phenological vegetation changes. We apply two principal quantitative methods, a multispectral image-differencing technique (described in Chapter 4), and topographic differencing. In each case, the difference data are presented as RGB color composites to highlight various features of the datasets. Image differencing portrays changed radiance as a function of changing materials or other physical changes on the surface, and topographic differencing portrays temporal changes in surface elevation over three time periods. The limited set of ground-based repeat photography presented here documents changes consistent with what has been discerned from repeat satellite images and repeated elevation mapping from airborne and satellite observations.

15.2 GEOLOGIC AND CLIMATIC CONTEXT

Hoodoo Mountain is a dormant, ice-capped peralkaline volcano (primarily trachyte and phonolite) in the Coast Mountains of northwestern British Columbia. Readers are referred to Chapter 14 of this book by Wheate et al. for a broader regional context and an overview of glacier changes in the western Canadian Cordillera.

The area has a maritime glacial climate, though it is intermediate between fully coastal maritime and continental climates. Several outlet valley glaciers, including Hoodoo and Twin Glaciers, flow from the Andrei Icefield (unofficially named[1]) centered ~16 km northeast of Hoodoo Mountain. Some of the outlet glaciers are relatively clean ice, while others are heavily debris covered.

[1] Andrei is the name of the son of Olav Mokievsky-Zubok, who did much of the glaciological work in the Coast Mountains in the 1960s and 1970s.

Hoodoo Mountain is a classic flat-topped, glaciovolcanic edifice (tuya) and largely formed when ice was much thicker within the massive Cordilleran Ice Sheet (Ryder and Maynard 1991, Edwards et al. 2002, Booth et al. 2003). Future eruptions of Hoodoo Mountain are likely, considering the mountain's Late Pleistocene history of eruptive episodes every 10^4–10^5 years. Although the most recent eruptions are post Last Glacial Maximum (e.g., less than about 10 kyr), the volcano shows no clear geophysical signs of imminent activity; eruptions in the near future are improbable, though possible. Any renewed eruption would result in lava–ice interactions with the volcano's ice cap, but would be less likely to affect Hoodoo and Twin Glaciers, which wrap partially around the base of the volcano and have a Pleistocene and Early Holocene record of lava interactions. Future summit eruptions from the ice-capped summit could produce phreatomagmatic activity (due to lava–water or lava–ice interactions) leading to widespread ash dispersal similar to the 2010 Eyjafjallajökull eruption in Iceland (Edwards 2010).

As a dormant peralkaline volcano, Hoodoo Mountain is lithologically and topographically different from most glacierized mountains in the Canadian Cordillera; it is one of half a dozen volcanic complexes with peralkaline lavas in central to northern British Columbia. This volcanic province is distinct from the dominantly andesitic volcanism of the subduction zones bordering much of the eastern Pacific Cordilleran belts. Besides being geologically young, Hoodoo Mountain has maintained a classic tuya form mainly because it has prominent, erosion-resistant lava flows at or near its summit. The ice cap and outlet glaciers to the north, including Hoodoo Glacier and Twin Glacier, occur on older rocks and over time have cut deep valleys. Supraglacial debris loads also are quite low, especially in comparison with many other places in the North American Cordillera (see Chapter 13 of this book by Kargel et al.).

The broader regional climatic and geological contexts are summarized in Chapter 14 of this book by Wheate et al. on western Canada, where a map of Hoodoo Mountain can be found (Fig. 14.1).

As a final contextual note, Hoodoo Mountain and other tuyas in British Columbia are features of special interest as terrestrial analogs of Martian subglacial volcanism (Edwards and Russell 2002, Smellie 2009, Martínez-Alonso et al. 2011) and as recorders of Pleistocene glaciations (Smellie 2009, Edwards et al. 2010). Continuing glacial retreat from the flanks of Hoodoo Mountain offers new possibilities for the study of fresh exposures of materials formed by ice interactions with a comparatively rare lava type.

15.3 SPECIAL TOPICS

15.3.1 ASTER image differencing

The ASTER sensor has produced excellent repeat image coverage of the Hoodoo Mountain ice cap and nearby Hoodoo Glacier and Twin Glacier, located about 250 km southeast of Juneau, Alaska, in the Coast Mountains (near 56.8°N, 131.3°W, northwestern British Columbia). Repeat satellite imaging of the Hoodoo Mountain area has enabled selection of two high-quality ASTER images acquired almost exactly one year apart (September 30, 2002 and October 30, 2003; Fig. 15.2), which we use to show changes between near-anniversary dates. These scenes have low percentages of cloud, haze, and snow coverage and were acquired with the same GLIMS gain settings to reduce image saturation over snow and ice; additionally, the nadir view angles are the same. The image pair differs by only three days in acquisition day of year and 85 seconds in time of day, so that the Sun has a similar position in the sky, thereby allowing application of the ICESMAP image-differencing method (see Chapter 4 of this book by Kääb et al.). Calculated with NOAA's online solar position calculator (*http://www.srrb.noaa.gov/highlights/sunrise/azel.html*), the Sun shifted by 1.08° in elevation; the cosine of the zenith angle (proportional to solar irradiance) decreased by 3.4%, and the solar azimuth shifted by only 0.06°, such that the directionality of shadows changed negligibly between scenes. Hence, the illumination fields of the two scenes are similar; this, coupled with the same sensor settings and near-anniversary date image acquisitions, greatly minimize both (1) spurious misleading image-to-image change signals that are reflective only of irradiance and scattering changes and are not reflective of true surface material changes, and (2) phenological vegetation changes. We note that our applications do not include albedo determinations or assessment of changing energy absorption at the surface.

With irradiance, sensor settings, and time of year controlled, there is no need for rigorous atmospheric corrections to reflectance space. This cir-

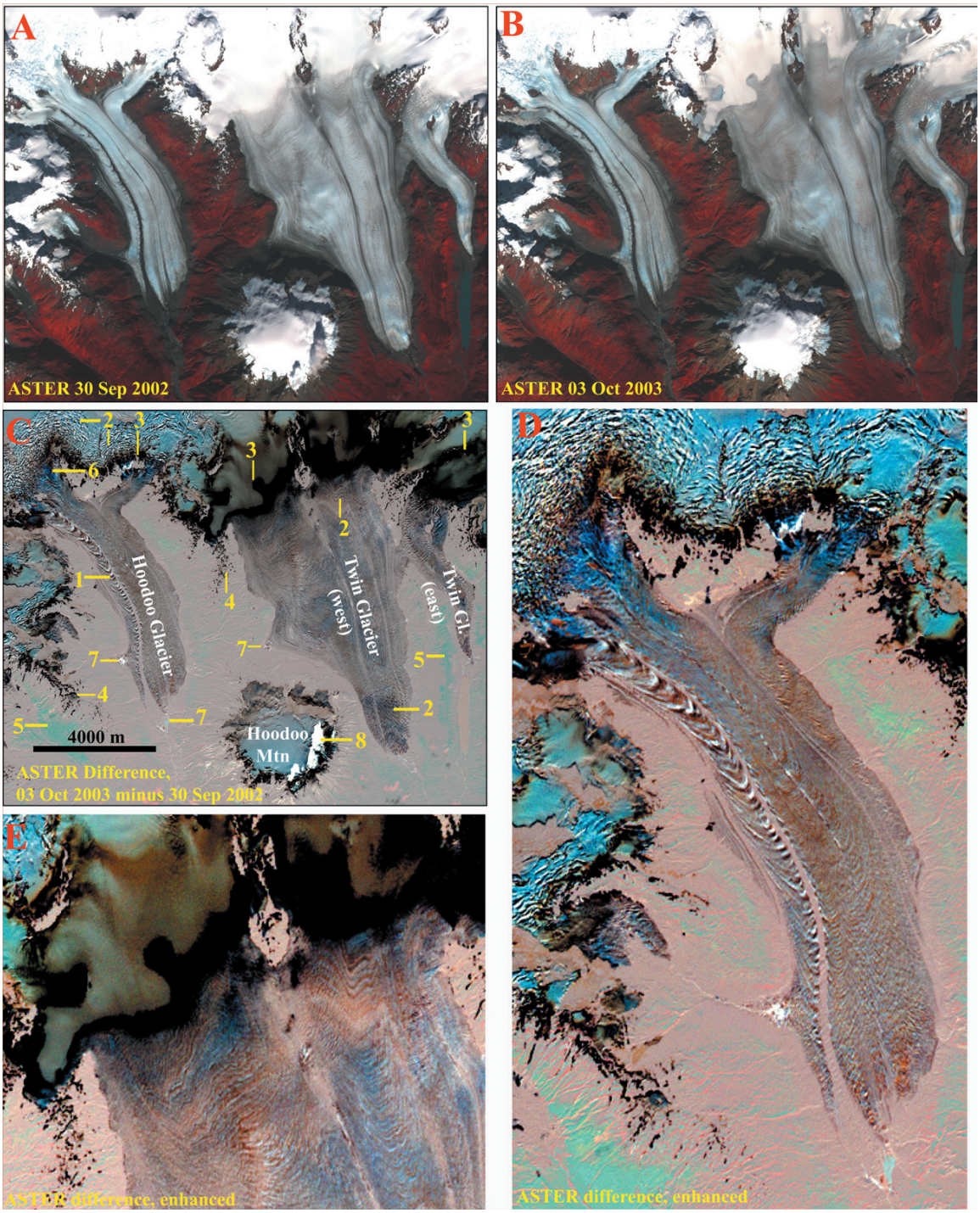

Figure 15.2. ASTER image differencing for a pair of ASTER images—RGB VNIR 321 scenes in top set of images (A, B)—acquired almost exactly a year apart. (C) Image difference, with the methodology of its production and a description of features indicated by annotations described in text. (D, E) Enlarged areas of image difference. The numbers in (C) represent: 1—ogives; 2—crevasse fields in the accumulation zone of Hoodoo Glacier and near the toe of Twin Glacier (west), and exposed layering near the top of the ablation zone of Twin Glacier; 3—area of decreasing transient snowline; 4—disappearing snow patches; 5—vegetation changes; 6—exposure of blue-ice fields; 7—changes occurring in lakes; 8—cloud cover differences. Readers should consult the Online Supplement for high-resolution versions.

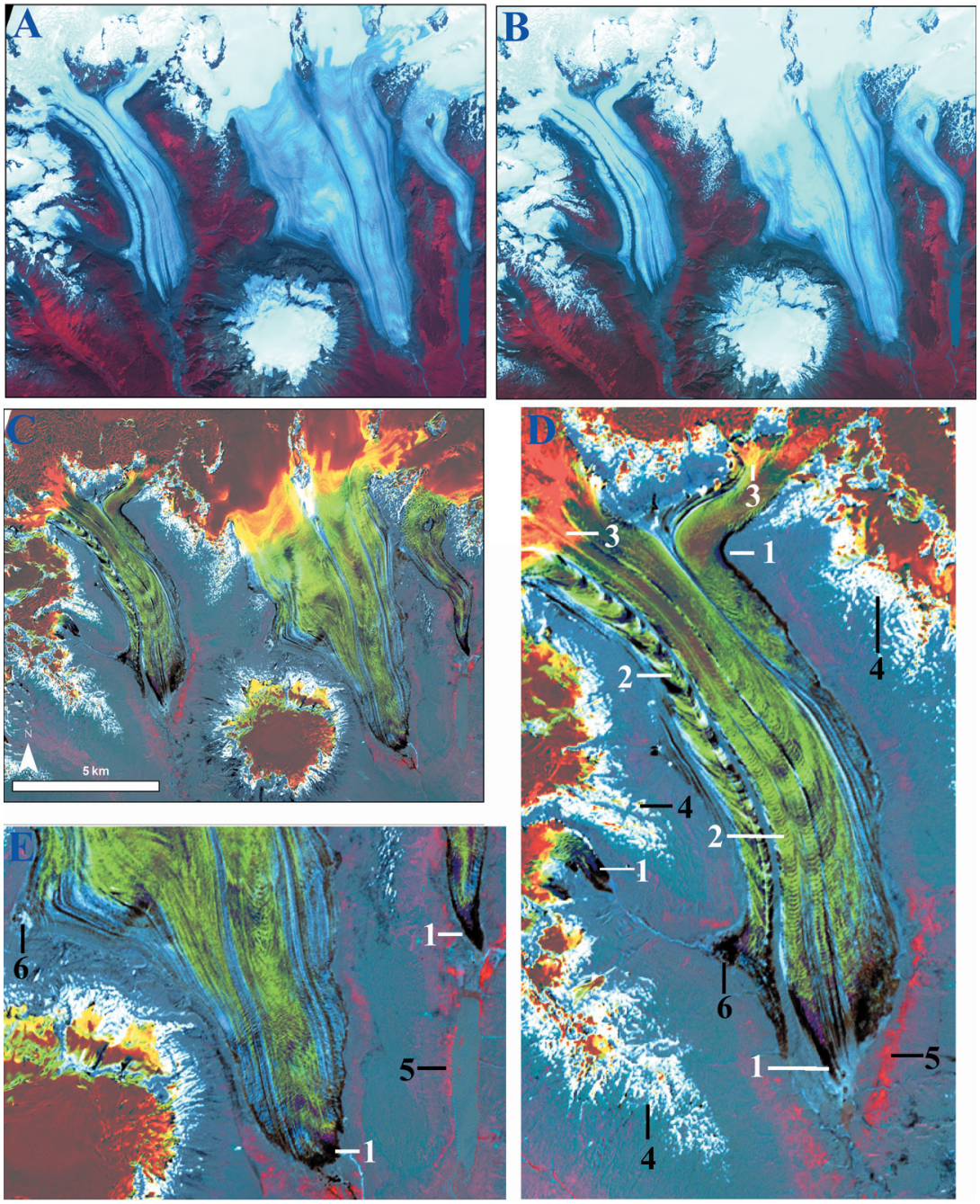

Figure 15.3. ASTER image differencing for a pair of scenes spanning 7 years (top pair). (Bottom left) The differencing product, described in text. (Panels at lower right) Some details of the differencing product. Numbers identify the following changing features: 1—glacier terminus and margin retreat (brown and black); 2—ogives; 3—advancing (lowering) transient snow areas; 4—new snow patches; 5—vegetation growth and primary succession; 6—ice-marginal lakes.

cumstance permits evaluation of glacier changes over a one-year period by simple subtraction of the 2002 image from the 2003 scaled radiance image. We used the AST14DMO product, which includes 15 orthorectified ASTER Level 1B calibrated radiance at sensor images (note that radiance values for ASTER Level 1B VNIR–SWIR products are rescaled into 8-bit data values; Abrams et al. 1999). Fig. 15.3 (see also Online Supplement) shows the subtraction image that has been rescaled

so that all DN values of the change scene are positive, such that an unchanging pixel has a neutral gray color.

Although the solar positions in the image pair are similar, they are not identical, resulting in a decrease in overall irradiance by 3.4% (from the cosine of the zenith angle). The decreased solar elevation caused the shadows of high peaks to lengthen; for example, a 500 m local peak would have a shadow lengthen by 39 m, or 2.6 ASTER VNIR pixels. However, shadows of relief features (including shadows cast onto glaciers), would lengthen by hundredths or tenths of a pixel (i.e., fairly insignificantly).

Another pair of ASTER images was similarly acquired close to anniversary dates, but seven years apart (Fig. 15.3). The gain settings for this pair were not ideal for ice and snow imaging due to their acquisition without use of GLIMS gain settings; therefore, snow is almost entirely saturated in VNIR bands 1, 2, and 3, and bands 1 and 2 are saturated in exposed ice areas, yielding a cyan color in RGB false-color 321 color composites. Subsequently, the heavily saturated conditions provide diminished resolution of features in snow and ice areas of the image compared with when GLIMS gain settings are used. This pair was acquired August 9, 2003 and July 27, 2010, thus differing by 13 days in acquisition day of year, and 42 seconds in time of day. The longer day-of-year difference and greater presence of extensive saturation compared with the 2002/2003 pair makes this 2003/2010 pair less well suited for the ICESMAP method, though it still yields a useful difference image of accumulated changes over a longer period (Fig. 15.2 and Online Supplement). This image pair has the Sun shifting by 1.07° in azimuth and 3.22° in elevation; irradiance increased by 5%. The likely difference in the radiance-at-sensor values has the effect of slightly brightening the difference image, and the solar elevation difference shifts the shadow of a 500 m mountain peak by 48 m, or about 3 ASTER VNIR pixels; a 70 m relief feature on a glacier would have a shadow shifting in length by 7 m or about 0.5 pixels.

15.3.1.1 2002/2003 image pair: A record of annual changes

Before image differencing, a subsetted pair of ASTER images was cropped around Hoodoo Mountain, Hoodoo Glacier, and Twin Glacier. Twenty manually selected ground control points were identified and, after applying a linear fit, the RMSE for image co-registration is submeter (<1/15 pixel). In the discussion that follows, we refer to the colors as rendered in the false-color 321 RGB image pair (Fig. 15.2A, B) and the difference image (Fig. 15.2C).

Well-correlated unchanging features within an ideal image pair contain image grid cell values that, when differenced, equal or approach zero. After rescaling so that difference values span the 0–255 (8-bit) DN space, these unchanging areas (e.g., mountain crests, slopes, valleys, and rock outcrops) should appear neutral gray. This can be seen in the differenced image (Fig. 15.2C), where most non-snow non-ice areas are gray and lack "texture" (i.e., they lack spatially alternating spectral response). In contrast, specific surface changes appear as variable combinations of distinct hues and textures such as the following:

(1) *Ogives* are rhythmic, commonly annual surface waves and are typically traceable upglacier to icefalls. Their origins reflect the influential components of topography, ice microstructure, and seasonal distribution of crevasses and local mass balance. A distinct ogive train occurs on Hoodoo Glacier (Fig. 15.2A, B). This ogive train shows roughly 20 ogive wavelengths per 5 kilometers of glacier length, thus indicating a flow speed in that sector of roughly 250 m/yr (slowing downglacier), assuming annual periodicity. If ogives were perfectly preserved downglacier, exactly annual, had perfectly uniform amplitude and wavelength, and were imaged at exact anniversary dates, then they would cancel and disappear in an annual difference image. Instead, Fig. 15.2(C, D) accentuates the ogives in Hoodoo Glacier, showing the train as a high-contrast pattern, resulting from imperfections or disparities within one or more of the classic ogive characterizations noted above.

(2) *Other possible ice dynamics features*: Some bright and dark, gray and brown mottled patterns or patches are identified, in some cases, with spatially resolved crevasses. Other patches may be unresolved crevasse fields or assemblages of thermokarst pits or other structures. The difference image shows some patches brightening and some darkening, thus contributing to a mottled pattern. To appear in the difference image requires some change occurring between the two images, but flow

displacement of unresolved features would not cause the observed change. One possibility is that a crevasse field could darken if the crevasses opened or became more numerous (letting light into the crevasses and disappearing in the glacier's interior), or it might brighten if crevasses partially closed; a heavily debris-covered glacier could brighten if crevasse formation disrupted the debris and exposed more ice on the surface. In the accumulation zone (cyan in Fig. 15.2C) larger crevasses are well resolved, and so flow displacement is sufficient to make individual crevasses appear in the difference image. Thermokarstic ice cliffs and giant moulins might be marginally resolved; no doubt their movement contributes to the fine mottled gray and brown ablation surfaces in the difference scene. Increased dust and decreased blue-ice exposures (especially near icefalls) might explain why glaciers darkened at some places.

(3) *Snowline and accumulation areas*: The sinuous black band represents a rising snowline. Areas of glacier ice that were covered with snow in 2002, but in 2003 became snow-free ice, appear black in Fig. 15.2C. These areas are revealed in the difference scene, but the difference image includes the influence of partial image saturation. These colors are not thought to represent dramatic changes other than interannual movement of the snowline.

(4) *Melted snowpatches* are indicated by black specks near but not on the glaciers.

(5) *Vegetation changes*: Some patches on nonglacier areas are turquoise in Fig. 15.2C, F, which may indicate decreased vegetation vigor, perhaps due to fires, disease, or droughts. However, most of the nonglacier regions exhibit a light gray–pink hue. This resulted from slight positive difference values in the NIR band 3 image pair (relative to band 1 and 2 differences), which indicates small changes in vegetation intensity (e.g., leaf area index or other indicators of plant vigor or species assemblages). The other contributory bands within the difference image, ASTER bands 1 and 2, are basically unchanged from the earlier and later images. The slight pink hue of the gray background is thus affiliated with slight vegetation differences, perhaps due to interannual phenologic variability (e.g., increased leaf area index in 2003 or delayed autumn senescence compared with 2002).

(6) *Icefalls* are cobalt-blue in Fig. 15.2(C, E) which may be due to removal of snow cover that had been present in 2002 and increased exposure of blue glacier ice in 2003.

(7) *Glacier lake dynamics*: The terminus of Hoodoo Glacier shows the development of a new lake or refilling of a previously drained basin (Fig. 15.2D). The lake is ~100 m wide, ~350 m long, and appears faint blue on the change image. The quasi-anastomosing (braided) morphology of the new lake indicates that the feature may be an area of actively flooding, shallow outwash. A small ice-marginal lake on the west side of Hoodoo Glacier (white in Fig. 15.2D), possibly drained in both images, is likely made visible by more numerous and shifting icebergs and a shifted calving front. A smaller similar lake appears on the west side of Twin Glacier's tongue but shows up as a mottled white-and-brown pattern, again likely resulting from changes in iceberg distribution. Field photos (discussed below) of an ice-marginal lake along the west-central side of Twin Glacier document periodic, likely seasonal drainage events.

(8) *Clouds* occur on the eastern and southern flanks of Hoodoo Mountain over snowy and vegetated surfaces in the 2002 image (Fig. 15.2C), and were absent in 2003.

15.3.1.2 2003/2010 image pair

A second multispectral ASTER image pair spanning seven years also indicates a host of surface changes (Fig. 15.3). Unfortunately, sensor gain settings for this pair were suboptimal; consequently, VNIR bands 1 and 2 are saturated over snow and ice. Differential but severe conditions of saturation have produced the gaudy colors in the difference image in the glacier areas and, furthermore, this pair is not as close to anniversary dates as the 2002/2003 pair. These problems render the difference image more difficult to interpret. Nevertheless, the 7-year time span and identical sensor gain settings provide an opportunity to extract useful decadal-scale surface change information using the ICESMAP image-differencing approach. Twenty-one manually selected ground control points were identified and a third-order polynomial fit was applied, yielding a submeter co-registration RMSE. The resulting difference image (Fig. 15.2C) has a different set of color patterns than in Fig. 15.2C partly because of actual differences in the change dynamics over seven years versus one year,

partly because of the image problems noted above, especially differences in partial (band-dependent) image saturation, and also because of the opposing shifts in terrain irradiance related to the particular dates of image acquisition. Note that in Fig. 15.3, the annotated numbers do not correspond to the same feature types shown in Fig. 15.2. Change features in Fig. 15.3C (enlarged in panels D–H) include:

(1) *Terminus retreat*: The black or brown tips and thin black or brown margins of each glacier in Fig. 15.3C show roughly similar magnitudes of terminus and marginal retreat; in each case, terminus retreat falls within the range of about 210–380 m (30–55 m/yr average). Hoodoo Mountain's ice cap is an exception, showing almost no indication of change in the satellite data, other than in transient snowline. Estimates of terminus retreat via comparison of mapping in the 1920s by Kerr (1948) to present day locations for the terminus of the eastern lobe of Twin Glacier give a comparable retreat rate of ~40 m/yr. Hence, the 2003–2010 period seems to be a linear extension of what has been happening since the 1920s, notwithstanding significant possible variations within that period. However, as we document in Section 15.3.2 below, thinning has actually accelerated.
(2) *Ogive field*: See discussion in Section 15.3.1.1.
(3) *Descended snowline*: The snowline in the 2003 difference image (Fig. 15.3C) is interpreted to be the contact between maroon (accumulation area) and yellow. The 2010 snowline is interpreted to be the contact between yellow and green (ablation area in both years). The yellow field thus represents the ablation area in 2003 but snow in 2010. However, the 2010 image shows many snow patches outside the glacier and a diffuse snowline on the glacier, which suggest that midsummer snowfall affected the 2010 image.
(4) *New snowfields* (white), not present in 2003, appear outside the glaciers in the 2010 image.
(5) *Vegetation* activity increased in 2010 on young moraines and outwash. These areas appear as red-hued zones (in ASTER 321 RGB color space). Vegetation may have grown and spread on these young postglacial deposits between 2003 and 2010.
(6) *Lake dynamics*: The small ice-marginal lake on the west side of Hoodoo Glacier appears black in Fig. 15.3E, probably due to drainage and melting of icebergs. By contrast, the opposite occurred to the small ice-marginal lake on the west side of Twin Glacier (Fig. 15.3G), probably indicating the presence of freshly calved ice in 2010. In panel H of Fig. 15.3, the northern end of a proglacial lake could be a prograding fan or delta, or reworking of thermokarstic sediment, with some attendant vegetation growth or succession.

15.3.2 Topographic differencing of Hoodoo Mountain and vicinity: Analysis of four time series of DEMs

Fig. 15.4(A–D) displays a sequence of four shaded relief DEMs for 1965, 1982, 1999, and ~2005. The intervening time period is 17 years for the first and second DEM pairs, and approximately only ~6 years for the last pair.

The 1965 DEM was produced from aerial photography and is from Canada's National Topographic Database (NTDB, *http://www.canmaps.com/topo/places/j/jcugt.htm*). The 1982 DEM also was produced from aerial photography and is from British Columbia's provincial Terrain Resource Information Management (TRIM) program. The 1982 DEM suffers from artifacts in the accumulation zone due to image saturation. Striping across Twin Glacier in the 1982 DEM is likely related to photogrammetric data compilation by different companies. The 1999 DEM is from SRTM and has lower resolution (90 m) than the other datasets but is consistent across the glacier surfaces. The ASTER DEM is a subset from the GDEM 1 global product, a mosaic compiled from numerous individual ASTER DEMs acquired between 2000 and 2008, and therefore carries a general temporal timestamp of about 2005. GDEM 1 has a pockmarked appearance, containing the pit-and-hill artifacts that typify this product.

The DEM sequence documents continuous glacier retreat and downwasting. The first pair shows separation of a tributary glacier from the west side of Hoodoo Glacier between 1965 and 1982. Cumulative downwasting from 1965 to ~2005 is quantified in Fig. 15.4E, where yellow and red hues show computed elevation loss, and blue shows computed elevation gains. We note that the zero (= balance) for the color scheme shown is in the light-blue zone. As Fig. 15.5 shows, nonglacier areas are very close to an unchanging

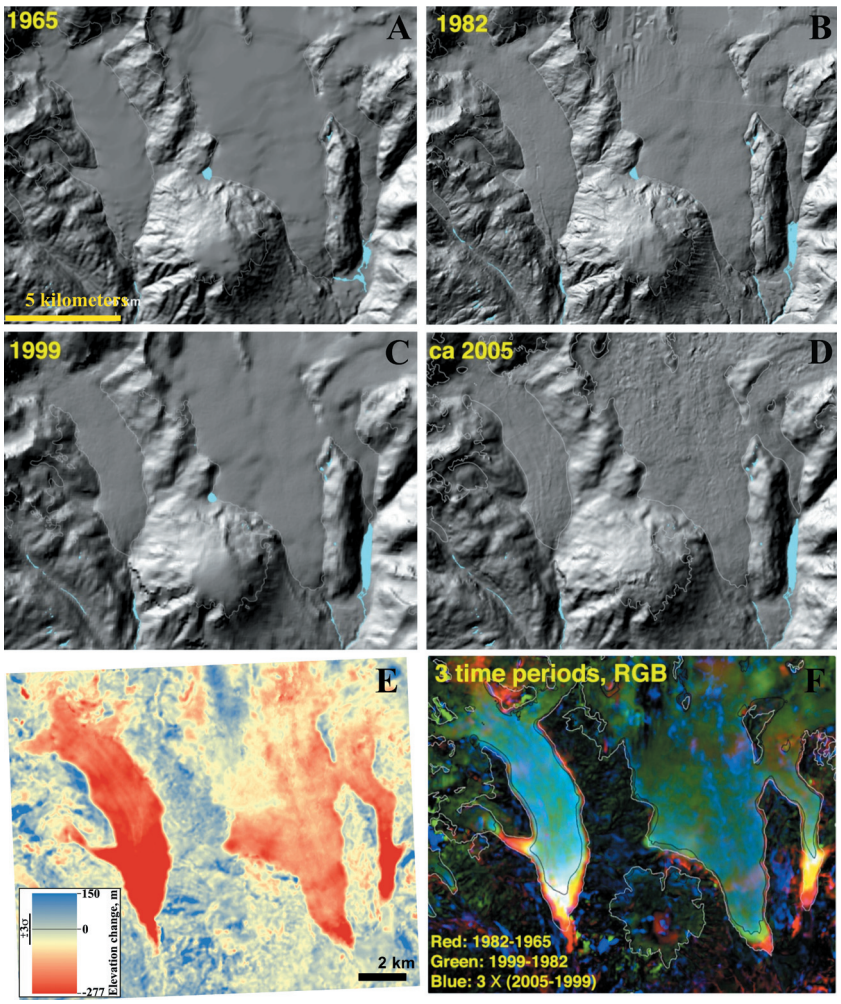

Figure 15.4. Four digital elevation datasets (A–D). Sources given in the main text. (E) Elevation differences of most recent minus earliest dataset. The color scale shows a $\pm 3\sigma$ measurement error range defined by the standard deviation of nonglacier areas (see Fig. 15.5); thus, values that show as peach, orange, or red represent significant thinning, whereas yellow to medium blue fall within a 3σ error range of zero (balance). (F) The four elevation datasets represented as differences occurring over each of three time periods: red—changes represented by 1982 minus 1965 DEMs; green—changes during the 1999 minus 1982 DEMs; blue—three times the change during the most recent time period, ~2005 minus 1999. The multiplier of 3× for the latest time period is to account for a briefer period compared with the earlier two time periods. Red and yellow represent areas of glacier retreat. The glacier tongues are mainly blue and green, indicating faster thinning during the later time periods than during the earliest one. Overall dark tones in nonglacier areas, and also on Hoodoo Mountain ice cap indicate little to no thinning (or thickening). Scene width ~16 km.

elevation, whereas glacier areas (mainly red in Fig. 15.4E) have thinned. Fig. 15.4E has not had bias correction applied (unlike Fig. 15.5, from which mass balance was assessed with bias correction implemented). Thinning is at a maximum in the lower part of Hoodoo Glacier. For the most part, glacier ablation zones have lost a few tens of meters in that period.

In contrast to significant elevation losses in all of the valley glaciers, and small losses in the accumulation zones, the Hoodoo Mountain ice cap shows very little change based on the DEM data. In 1997, Russell et al. (1998) used ice radar to determine whether the central part of the ice cap was less than 200 m thick, and the DEM analysis seems to support this as a relatively stable long-term characteristic. We show in Section 15.3.3 that field-based photography has identified areas where thin-

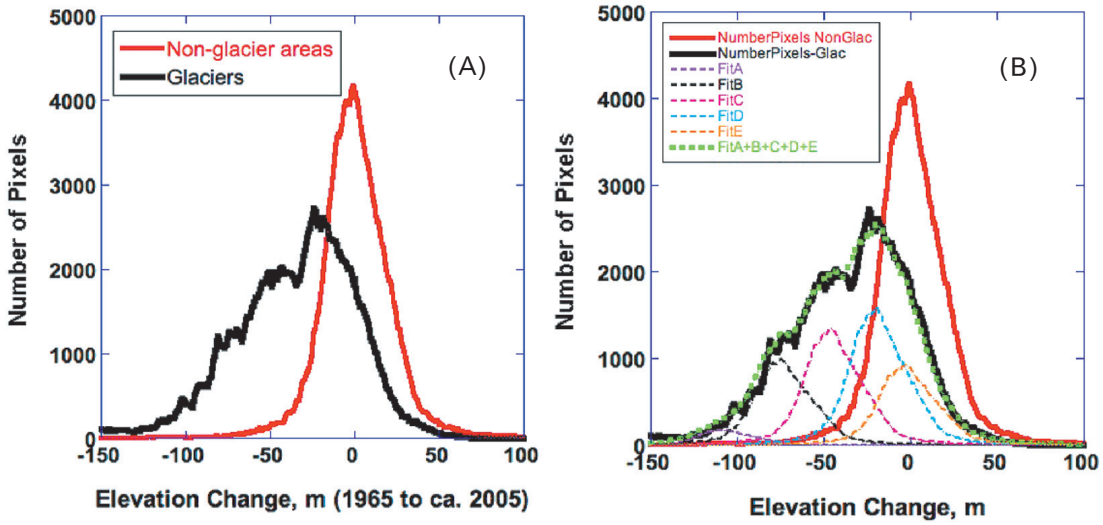

Figure 15.5. Histograms of elevation change of the ~2005 GDEM 1 minus the 1965 NTDB DEM in the Hoodoo Mountain area that was shown in Fig. 15.4. Glacier and nonglacier areas are compared in (A), where a small bias has already been removed, as discussed in the text. The nonglacier curve basically represents the measurement error function, since no areas there are likely to have changed elevation significantly. (B) The same two observational curves together with a set of five functions that have then been added together to simulate the glacier elevation change function, as discussed in the text. The five individual functions are of exactly the same form as the nonglacier curve but have been shifted in amplitude and mean; the dotted green curve is their summation. The average elevation change of the glacier areas amount of a mean of −37 m over 40 years between measurements (−0.94 m/yr). Curve fit components include 40-year means of curve A (not readily visible but needed to match the long negative tail) = −108 m (−2.70 m/yr), B = −75 m (−1.88 m/yr), C = −46 m (−1.15 m/yr), D = −20 m (−0.50 m/yr), and E = −3 m (-0.08 m/yr).

ning has occurred, but apparently it was not enough to be resolved in the DEM analysis.

Fully exploiting the fact that we have four DEMs representing three time intervals, we rendered the three DEM differences as a color RGB image (Fig. 15.4F), where the red band represents elevation change during the first interval (1965–1982), green for the second period (1982–1999), and blue for the third period (1999 to roughly 2005 on average). The "blue band" is weighted by a factor of 3 to account for the shorter interval represented. This rendering shows where thinning has decelerated (yellows and reds), where it has been intense and constant (white areas), or where it has accelerated (turquoise and blue areas). In general, the image shows that thinning has accelerated over the glacier tongues, except that the glaciers fringes are represented in red and yellow tones because their margins retreated beyond those areas by the time the later data were acquired. Fig. 15.4F also shows that thinning extends up to about the late season snowline or equilibrium line.

Another representational approach is to plot the changes of elevation as histograms, with glacier and nonglacier areas isolated for comparison (Fig. 15.5). Nonglacier (unchanging or nearly stationary) areas should theoretically not show significant elevation change. Rather, these areas in aggregate show what is interpreted to be a −3 m bias in the computed mean elevation change over the 40-year period between observations (−0.075 m/yr). Bias correction has been applied in Fig. 15.5 by adding 3 m to all values shown. Nonglacier areas have an approximate Gaussian normal distribution of changes, which reflects the error distribution function. Fig. 15.5 shows a clear net average elevation change of −37.4 m of glaciers—averaging −0.94 m elevation change (thinning) per year—compared with nonglacier areas. Glacier areas taken as a whole have a strongly negatively skewed, non-normal distribution of topographic changes, which is indicative of real variations in the amount of thinning. Thinning varies between glaciers, which is partly reflected both in the multimodal distribution (Fig 15.5B) and in the pattern of thinning shown in Fig. 15.4E. We have fit the glacier-thinning distribution using five co-added loss values, each having the same error distribution as

nonglacier areas but shifted to various negative values. The closeness of fit suggests that each major glacier ablation area (Hoodoo, East Twin, West Twin, and Hoodoo Mountain) and the collective accumulation zones tend to have a discrete negative balance but share the same measurement error function as shown by nonglacier areas. Of course, this is just a mathematical approximation but indicates that different glaciers have thickness losses ranging from near balance (Hoodoo Mountain's ice cap and the collective accumulation zone) down to −2.70 m/yr. This method of assessment allows us to discern average elevation changes with a precision of 0.25 m/yr (approximated as 3 times the bias rate of 0.075 m/yr), though in this case use of GDEM 1 introduces ambiguity in the number of years represented.

The average thinning rate we have found, −0.94 m yr^{-1}, compares closely with that reported previously by Schiefer et al. (2007) for the Andrei Icefield; those authors reported a change of −1.1 m yr^{-1} for the period 1985 to 1999. They also found a mean elevation change rate of -0.78 ± 0.19 m yr^{-1} for the same period for ice throughout British Columbia, and -0.83 ± 0.19 m yr^{-1} for just the northern Coast Ranges. The reporting periods differ from ours, and our study area covers just the southern half of the Andrei Icefield plus Hoodoo Mountain.

The average thinning rate for the study region also compares very closely with that determined by Shea et al. (2012) in the 2000–2007 period for the Sittakanay Icefield about 100 km north. Those authors used two methods (geodetic and a MODIS snowline-based technique) and found elevation change rates averaging −0.68 and −0.90 m yr^{-1} for these two methods. Our value of −0.94 m yr^{-1} for our study area pertains to a longer time interval (1965 to ∼2005).

Despite the differences of the various time periods and areas considered in our work and those of Shiefer et al. (2007) and Shea et al. (2012), there does appear to be province-wide coherence of sustained and probably accelerating thinning throughout the Coast Ranges. Shea et al. (2012), however, report a much slower thinning rate in the interior Columbia Icefield of the Rocky Mountains; slower thinning there is consistent with that area's more extreme, drier continental climate, lower precipitation rates, and lower mass turnover. The broader regional picture of glacier fluctuations in the BC Coast Ranges is further treated in Chapter 14 of this book by Wheate et al.

15.3.3 Mass balance of glaciers in the Hoodoo Mountain study region

The elevation changes recorded on glacier areas relative to presumed unchanging nonglacier areas (Fig. 15.5) can be converted to estimates of mass balance. We assume a mean glacier ice density of 890 kg m^{-3}, which is consistent with 3% bubble porosity and a constant macroscale porosity (such as crevasses and empty moulins) as the glaciers thin. The overall average mass balance of the combined set of glaciers in the study region so calculated was about −840 kg m^{-2} yr^{-1} from 1965 to about 2005, though different glaciers or parts of glaciers have specific mass balances ranging within an error of zero (in balance) to −2,400 kg m^{-2} yr^{-1}. Furthermore, the documented increase in the rate of thinning (Fig. 15.4F) indicates an increased magnitude of negative balances over the four decades of the study period, and by now it could well be greater than the average we calculated.

Errors in the average mass balance over the entire four-decade period include uncertainty in the mean date of the GDEM 1 used in the ∼2005 ASTER DEM (estimated as ±2 years, thus contributing 5% error to the mean mass balance or ±42 kg m^{-2} yr^{-1} error); uncertainty in the porosity of ice and its density (estimated as 3% error or ±25 kg m^{-2} yr^{-1}); and uncertainty in the bias correction (estimated as about half the value of the bias correction, or about ±34 kg m^{-2} yr^{-1}). The standard error of the means—assuming Gaussian distributions of elevation change determinations (Fig. 15.5)—of nonglacier and glacier areas is negligible due to the large number of elevation cells in the DEMs. The error components are uncorrelated, so that the combined error is the square root of the sum of the squares of the errors, calculated as ±60 kg m^{-2} yr^{-1}. Mean mass balance, with rounding to two significant figures and error tripled to 3σ, is thus -860 ± 180 kg m^{-2} yr^{-1} for the period 1965 to 2005. 3σ should account for other errors that might be hidden in areas of the glaciers where parallax was not determined accurately in either dataset (e.g., due to snow saturation in some areas or to changing macroscale porosity.

15.3.4 Ground and air photo assessment of glacier changes on Hoodoo Mountain and vicinity

During five field seasons (1993, 1994, 1996, 1997, 2004) to examine volcanic deposits at Hoodoo

Mountain, the extents of glacial cover have also been documented on Hoodoo Mountain and locally for Hoodoo and Twin Glaciers (Edwards and Russell 1994, Edwards et al. 1995, 1999). General observations about the extent of glaciers and glaciation in the area were also made by Kerr (1948) and MacDonald (2006). Edwards et al. (1995, 1999) and MacDonald (2006) documented glaciolacustrine sediments in a small basin between the northwestern flank of Hoodoo Mountain and Hoodoo Glacier that are consistent with the glacier surface that existed approximately 670 calendar years before present, when they were up to 100 m higher than today. Our DEM analysis (Fig. 15.5) suggests that most of this thinning of Hoodoo Glacier occurred after 1965, but consideration of the rough map reported by Kerr (1948) indicates that terminus retreat was already well underway between 1929 and 1965. Observations between 1993 and 2004 were made via ground-based and aerial surveys (Figs. 15.7–15.10), and reinforce some observations made via satellite and DEM analysis, while also documenting some changes not as obvious from remotely sensed data.

15.3.4.1 Twin Glacier

Several changes to Twin Glacier have been documented by field-based studies over the past 90 years (Figs. 15.6–15.8). Based on mapping in the 1920s by Kerr (1948) and in the 1990s by Edwards et al. (1999), the terminus of Twin Glacier has retreated ~4 km over that time (averaging ~44 m/yr retreat). Mapping by Kerr in the 1920s showed that the southernmost part of Twin Glacier flowed around both sides of a north to south–oriented bedrock

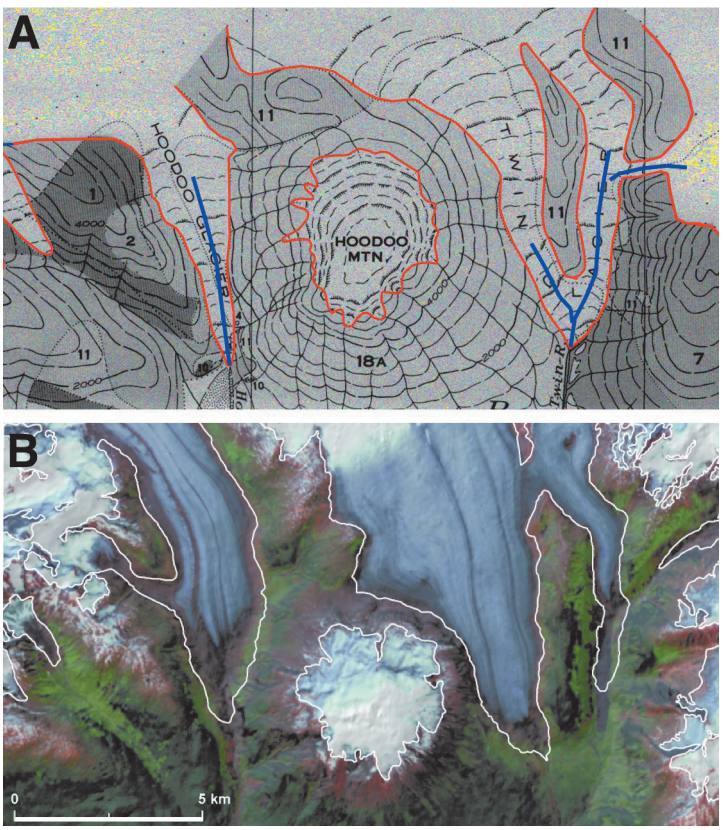

Figure 15.6. Long-term retreat of Hoodoo and Twin Glaciers, and the comparative stability of the margin positions of Hoodoo Mountain ice cap, are indicated here. (Top) A topographic sketch map suggests how far Twin and Hoodoo Glaciers have retreated since the map data were produced during the late 1920s (map by Kerr 1948). The blue lines are approximate pathways of subsequent retreat. Note that Twin Glacier is depicted true to its name, with two roughly coequal, coalescing branches of a large valley glacier system. (Bottom) Satellite image—Landsat TM 5 July 26, 2010 color composite 321—showing glaciers that have retreated, including the detached branches of Twin Glacier. White outlines indicate 1982 glacier extent. No quantitative comparison should be made between the top and bottom panels, but they do indicate that glacier retreat here has been ongoing from the early 20th century.

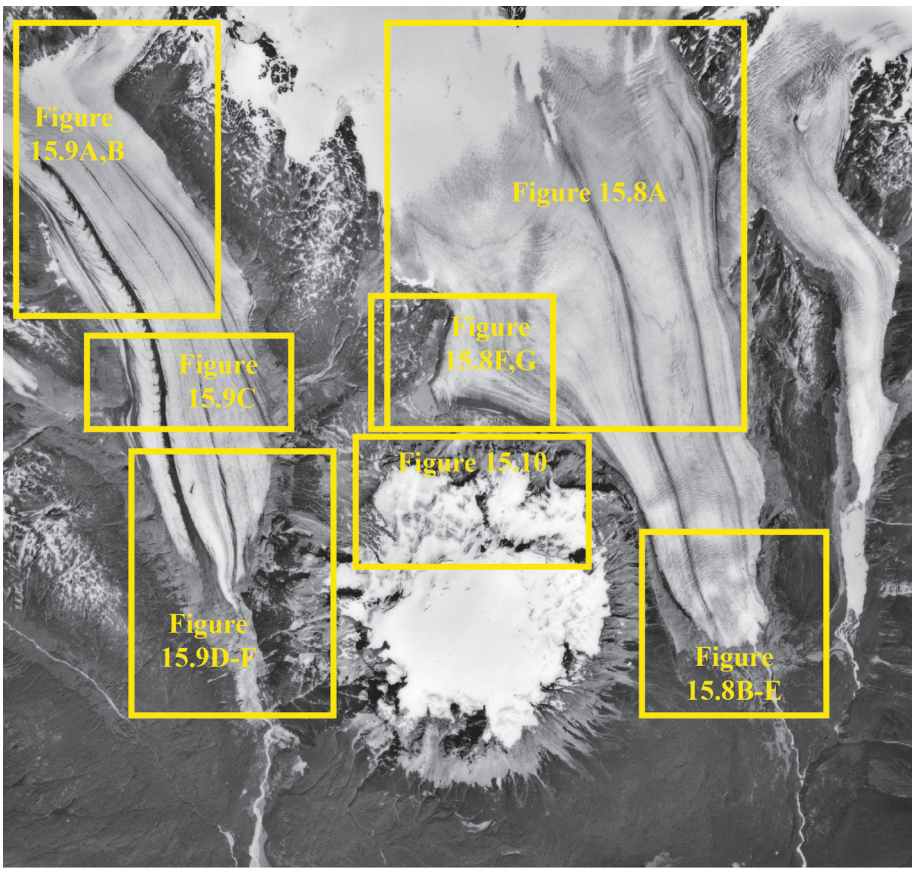

Figure 15.7. Aerial photo (BC82022_206) showing locations of ground and air images of Twin Glacier, Hoodoo Glacier, and Hoodoo Mountain.

ridge but was continuous to the south of the ridge. By the 1950s the glacier had retreated to the point where the terminus separated into two lobes, one east and one west of the ridge (Fig. 15.7). Short-term changes to the western lobe terminus are ubiquitous (Fig. 15.7B, C). However, the stepped and nonvegetated ground surface immediately in front of the terminus at the western lobe is a clear indication of rapid ice retreat in recent decades (Fig. 15.8D, E). Subtle changes to the glacier surface are evident farther to the north where, in midsummer, ice has been periodically exposed over the past 15 years.

Along the southwestern margin of the glacier, a small, moraine-dammed lake appears to drain annually along the moraine formed between the glacier and the northeastern side of Hoodoo Mountain (Fig. 15.8F, G). By careful comparison of the ice and lake edges relative to some terraces and other topographic features in Fig. 15.8(F, G), it is evident that the glacier surface at this site has lowered, and with it the lake level; in other ways the lake and adjacent glacier dynamics inferred by crevasses in the glacier and icebergs on the lakebed are very similar. Changes in the apparent debris cover on stranded ice blocks in the drained lake in 2004 (Fig. 15.8G) are consistent with periodic drainage events, although a full lake level has only once been observed in the field (1993).

15.3.4.2 Hoodoo Glacier

Field mapping has documented significant retreat of Hoodoo Glacier during the past 90 years. Comparison of Kerr (1948) and Edwards et al. (1999) shows a minimum terminus retreat of 2 km over the past 90 years (roughly 20 m/yr). In the 1920s the position of the terminus was ~4 km north of the Iskut River, and at present the terminus is ~6 km north of the same point (these numbers are approximate). ^{14}C geochronology analytical results on glaciolacustrine sediments in a valley adjacent to

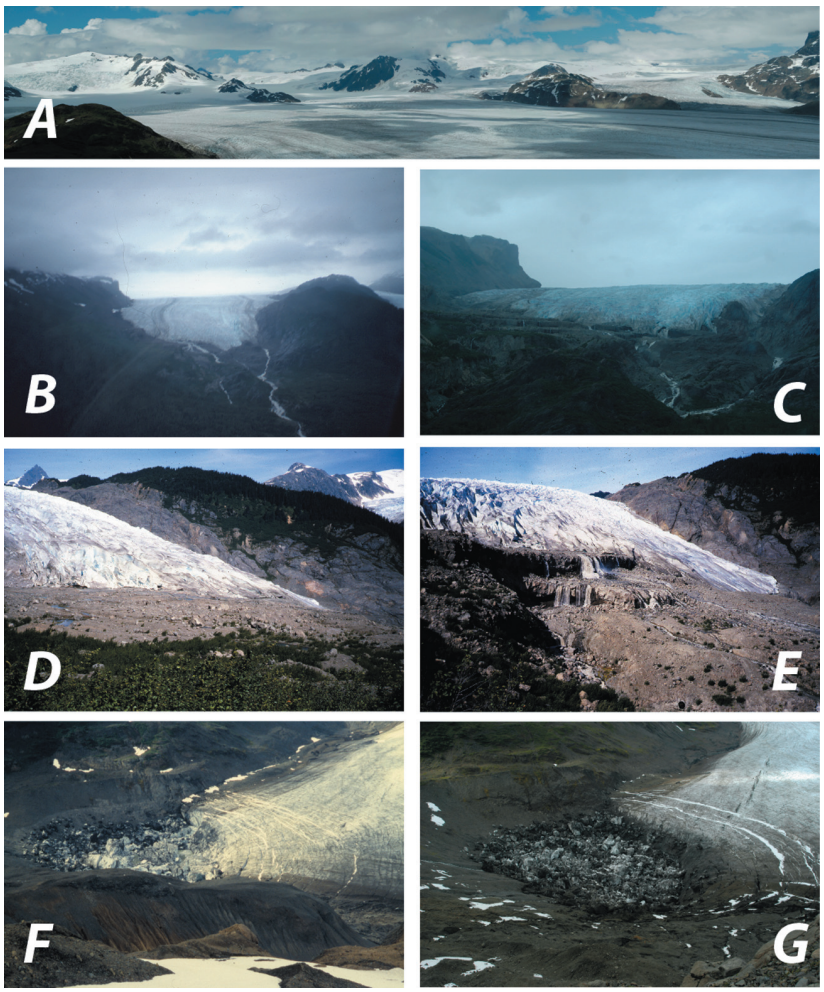

Figure 15.8. Images of Twin Glacier. (A) Panoramic view as viewed from Hoodoo Mountain looking to the north (images from July 2004). (B) Aerial view of the terminus of the western lobe in summer 1993 as seen from the southwest. (C) Same as (B) but taken in 2004 from a slightly different aerial location looking directly north. (D) Ground-based view to the northeast at the terminus of the western lobe (image from July 1993). Note the flat surface in middle ground where ice has recently retreated but vegetation has not yet returned. (E) Same as in (D), but view from the south, at the headwaters of Twin River (image from July 1993). Note stepped surfaces marked by waterfalls that have been cut into lava flows from the east flank of Hoodoo Mountain volcano (left). (F, G) Views of drained, moraine-dammed lake at the southwestern edge of Twin Glacier (F: July 1993; G: July 2004).

Hoodoo Glacier are consistent with ~100 m of net vertical lowering of the glacier surface over the past ~700 years (Edwards et al. 1999, MacDonald 2006), ~0.14 m/yr average. Hence, although overall glacier retreat and thinning has been occurring for centuries, quantitative comparisons of the rates indicate that thinning in the past several decades has been far more rapid than the average rate for the past 700 years. Indeed, the recent thinning rates of these glaciers, no different from those of most other western Canadian glaciers, could not be sustained for long before Hoodoo Glacier and other nearby glaciers would disappear. Comparisons of ice cover for a rock knoll at the head of Hoodoo Glacier between 1993 and 2004 (Fig. 15.9A, B) shows visual evidence of a reduction in ice cover over that 10-year period. Most of the length of Hoodoo Glacier is highly crevassed (Fig. 15.9C), with almost the entire length of the glacier being snow free by midsummer. Towards the terminus of the glacier, water drainage from the northwestern quadrant of the adjacent Hoodoo ice cap is directed along the margin of the ice, where Late Pleistocene/Holocene lava flows plunge below the glacier's margin (Fig. 15.8D). The terminus now hosts a small, well-drained lake (Fig.)15.9F).

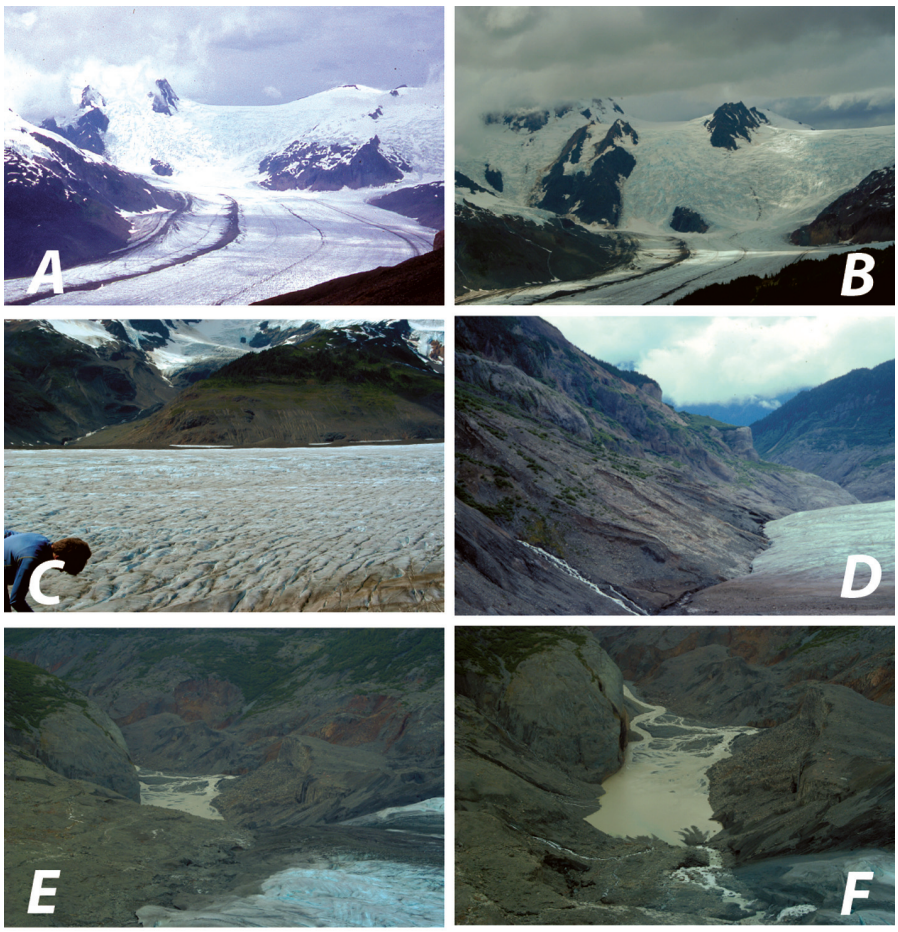

Figure 15.9. Images of Hoodoo Glacier. (A, B) Views upglacier to the northwest showing the icefalls at the head (A: 1993; B: 2004). (C) View to the west of crevasses (image taken in July 2004). (D) View to the south along the southeastern edge where lava flows from Hoodoo Mountain plunge beneath the ice surface (image taken in July 1993). (E, F) Views towards the south showing the terminus and the small moraine-dammed outlet lake (both images taken in July 2004).

15.3.4.3 Hoodoo Mountain ice cap

Hoodoo Mountain ice cap is approximately 3 km in diameter, and has a maximum thickness of ~200 m (Russell et al. 1998). Analysis of DEMs shows that the thickness of the ice cap has not changed significantly during the past decade. However, repeat field images of ice cap margins do show local areas of ice margin thinning and slight retreat (Fig. 15.10), although not nearly as much as at the termini of Twin and Hoodoo Glaciers and not enough to be resolved in ASTER imagery. This observation might be explained by the relative differences in elevation between the ice cap and the adjacent valley glaciers. Hoodoo Mountain ice cap mainly persists between 1,600 and 2,000 m in elevation, and so maintains at least partial snow cover during all months of the year. However, the much lower elevations of the tongues of Twin and Hoodoo Glaciers, along with possible local orographic effects from surrounding high mountains, both likely act to limit snow retention on those glaciers, allowing for greater ice exposure and melting during summer months. In Fig. 15.10 we show evidence of thinning of ice near the margins ranging between 16 ± 5 m and 20 ± 5 m, between 1993 and 2004, which equates to an average thinning rate of 1.5 ± 0.5 to 1.8 ± 0.5 m/yr. We have made comparable rough estimates of margin thinning at other points near the edge of Hoodoo Mountain ice cap; measured values are 0 ± 5, 8 ± 3, and 9 ± 3 m, which equate to rates of 0 ± 0.5, 0.7 ± 0.3, and 0.8 ± 0.3 m/yr. The average of the five measurements is 10.6 m/11 yr, or ~1 m/yr. However, we note only a few spots along

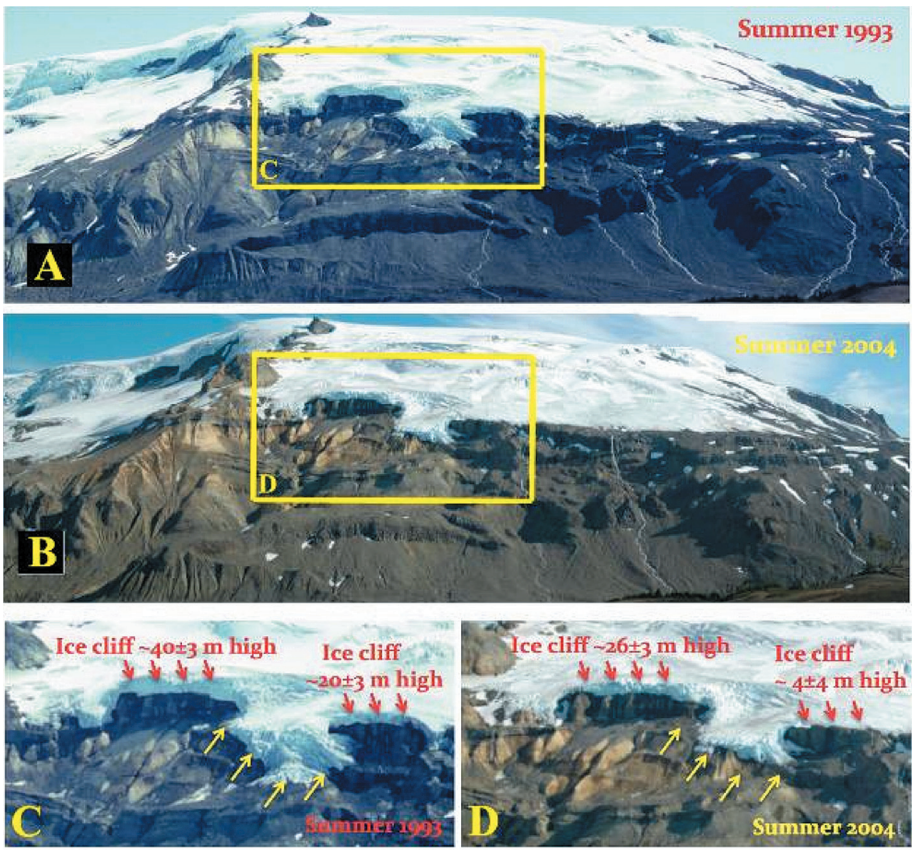

Figure 15.10. Images of Hoodoo Mountain and its ice cap. (A) View to the south from the north side of Hoodoo Mountain volcano (taken in summer 1993). Vertical scale is approximately 1,000 m from top of mountain to bottom of image. Yellow box shows approximate location of panel (C). (B) View also to the south from the north side of Hoodoo Mountain volcano (taken in summer 2004). Yellow box shows approximate location of panel (D). (C, D) Enlargements centered on the same ice tongue from the ice cap taken in July 1993 (C) and July 2004 (D). Obvious thinning, yet very little retreat during the 11-year period between images has taken place along the edge of the ice cap. Approximate thinning of the ice cliffs measured from these photos (scaled from the height of the mountain) in the two sectors marked by red arrows is 14 ± 5 and 16 ± 5 m (left to right side, respectively). Yellow arrows mark a more complex area where thinning of the ice near the margin of the ice cap also has occurred, but ice cliff geometry and underlying terrain are too complex to allow accurate measurements of ice thinning.

the edge of the ice cap where notable (but minor) retreat has taken place. It is no surprise then that ASTER image differencing identified almost no change of ice cap margins.

The set of four DEMs shows no significant thinning of Hoodoo Mountain ice cap. A possible explanation is that ablation is controlled largely by dry land calving off the cliffs at the edge of the ice cap. This process may buffer the position of the edge of the ice cap; if the ice made a slight advance and thickened along the margin, calving would increase and effectively counter the ice cap's attempted growth; conversely, thinning and slight retreat between 1993 and 2004, would cause a decreased rate of calving, thus minimizing the retreat. Thus, the shape of the landform controls the shape and extent of the ice cap, which responds to climatic fluctuations but with low sensitivity.

Fig. 15.11 is a stereo anaglyph to emphasize to readers the shape of Hoodoo Mountain, and the geomorphological distinction of that volcano and ice cap relative to the Andrei Icefield and its radiating set of valley glaciers. The anaglyph was prepared from a stereo ASTER scene acquired on October 3, 2003. This region presents a clear instance where the local geology and Pleistocene land surface processes (especially glaciation and volcanism) have produced two completely different mountain types having two completely different hypsometries, which now control distinctive types

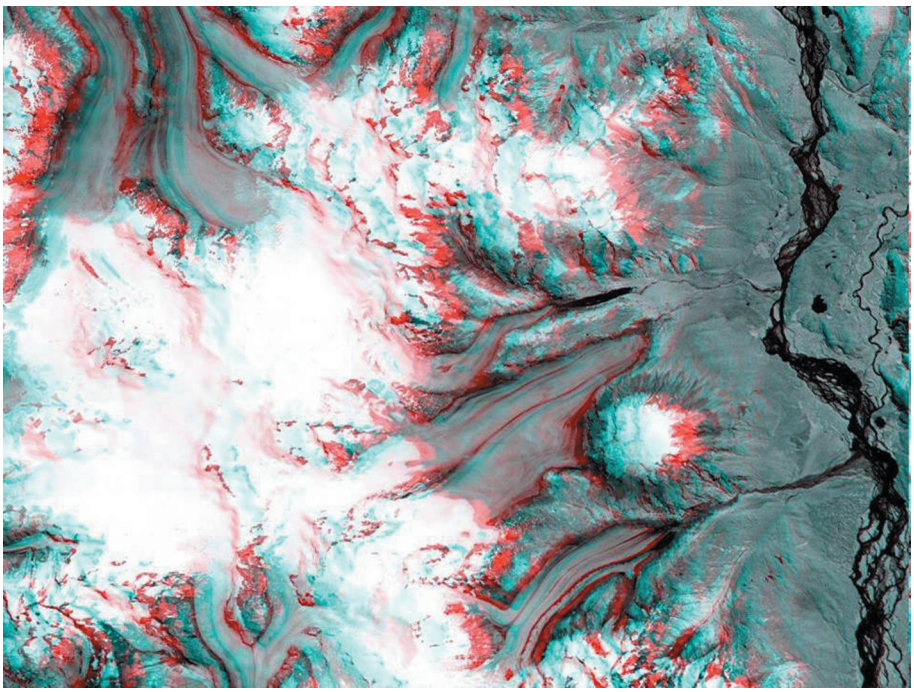

Figure 15.11. Stereo image anaglyph (requiring 3D glasses for proper viewing) generated from an ASTER scene acquired October 3, 2012. North approximately to the left. This cropped scene is about 29 km (top to bottom) × 33 km (left to right). Hoodoo Mountain is the distinct flat-topped volcano in the lower-right quadrant. The Andrei Icefield (informal name) dominates the northern (left) half of the scene, with the Andrei Glacier flowing east (up) from the icefield. Our study focuses on the south-flowing glaciers and the ice cap of Hoodoo Mountain.

of glaciers, which in turn are responding differently to climate change.

15.3.5 Glacier and climate changes in the vicinity of Hoodoo Mountain

15.3.5.1 Climate records

We have examined some key parameters from two climate records (Canadian Daily Climate Data 2007) of stations near Hoodoo Mountain and Twin Glacier (Fig. 15.12). The stations, Dease Lake (58.43°N, 130.02°W, ~800 m asl) and Stewart (55.95°N, 129.98°W, ~20 m asl), bracket the latitude and longitude of the Hoodoo Mountain and Twin Glacier area. Dease Lake station is 200 km northeast of Hoodoo Mountain, and Stewart station is 130 km to the southeast. The maritime climate of the Stewart station and the severe continental climate of the Dease Lake station also bracket the climate zone of Hoodoo Mountain and vicinity. The intermediate climate zone near Hoodoo Mountain is reflected in the elevations of NCglacier terminations in that area, mainly around 500–600 m elevation, versus those of glaciers in the nearest maritime zone (0–200 m) and the continental zone to the east (800–1,500 m terminations).

Both climate stations have undergone warming and increased precipitation over the duration of the time series (six decades long for Dease Lake and ten decades for Stewart). These climate records include some data gaps, including months where a few days of the record are missing. Where more than two days of data were missing, the entire month was deleted. For summer temperature records, if any one of the summer months (June, July, August, and September) were missing, then the entire year was deleted for purposes of linear and nonlinear regression analysis; we believe that a year's data gap is likely to introduce errors or bias less severe than if any summer month was missing (which would shift the summer average for that year far off the real average).

Recent warming rates can be assessed from the available records using different statistical treatments, especially in the choice of curve fit. For

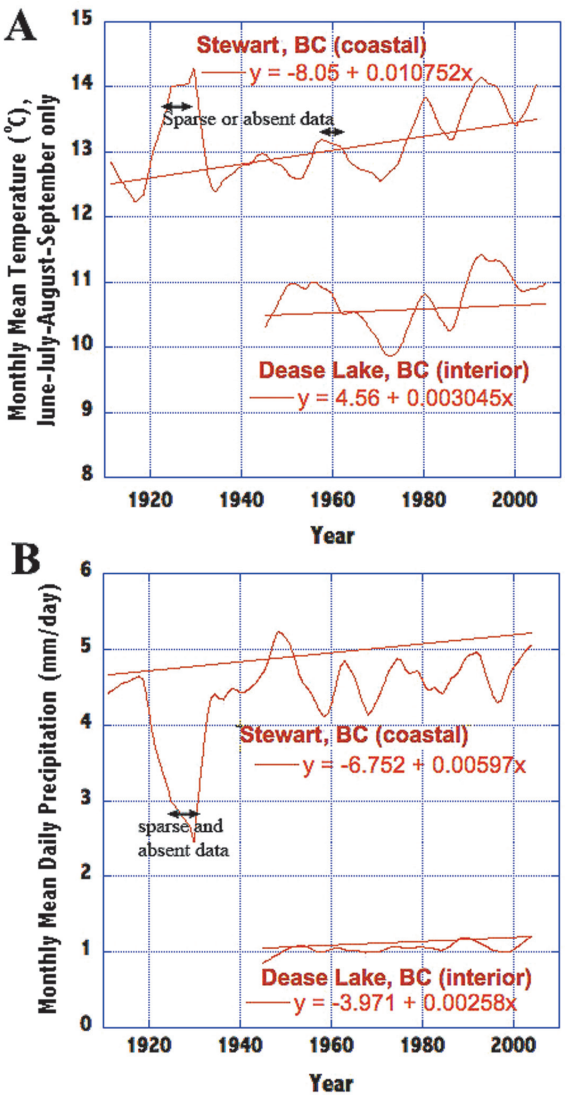

Figure 15.12. Dease Lake and Stewart, BC climate data records for summer mean temperature each calendar year (June–July–August–September mean temperature) and monthly mean daily precipitation, available online courtesy of Environment Canada's National Climate Data and Information Archive. These two weather stations represent a coastal maritime climate (Stewart) and an interior continental climate (Dease Lake) bracketing the location and presumably the climate of the Hoodoo Mountain area. The red lines are linear least squares fits (equations given) to show centennial-scale trends; the red curves are running decadal means to highlight decadal variability. All the linear trends have slopes that are statistically significant. Note that, because the oscillating curve is a running mean, the line is a least squares fit to the unsmoothed dataset (and thus is more sensitive to strongly skewed data; the precipitation for Stewart, in particular, has strong upward skewness due to years of extremely high precipitation).

Stewart, the linear fit to almost a century of data indicates a mean summer warming rate of 1.1°C/century, whereas a second-order polynomial fit (not shown in Fig. 15.12) to the same data gives a recent decades (latter 20th century towards the present) summer warming rate of 3.1°C/century. For Dease Lake, the six-decade record indicates a nearly flat linear warming trend of +0.3°C/century, though the second-order polynomial gives a recent rate of 2.5°C/century for the last couple of decades of the record. Thus, these records indicate warming, but lacking any model that incorporates other parameters of the climate system, including influences of the Pacific Decadal Oscillation, no reliability can be placed on the rate of warming due to anthropogenic causes. More data from other stations would have to be analyzed to extract a reliable climate time history. Nevertheless, the two stations' records show a strong coherence, especially since 1960, despite the significant climatic distinction between the two sites. We suspect that the linear trends probably underestimate recent warming, because the average rate includes periods before the time when atmospheric CO_2 increase began to have significant warming effects.

We considered other curve fittings, including a weighted moving boxcar fit (Fig. 15.12) that minimizes the influence of outliers. The Dease Lake record is too brief to lend any merit to nonlinear curve fits. However, a second-order polynomial, or piecewise linear curve fits, or almost any curve other than a single linear fit indicates that the Stewart record shows accelerating or stepped-up warming subsequent to 1970 compared with a flat or slight cooling trend prior to 1970. However, we do not assign any reliability to this more rapid recent warming, because the influence of decadal oscillations remains very strong and can confound attempts to extract higher order signals when the record is so short. Probably another 10–20 years of climate data will be needed to conclude with any confidence that warming is accelerating. For now, we can rely only on the century-scale warming seen in the Stewart climate record and the high coherence of decadal oscillations seen in both stations' records.

As for precipitation, linear fits indicate increases at rates of 22% and 11% per century for Dease Lake and Stewart, respectively (Fig. 15.12). However, the precipitation trends are highly uncertain, largely because the curve fits are affected by high upward skewness (i.e., some years when precipitation was exceptionally high).

15.3.5.2 *Inferences for glacier response times*

The effects of increases in precipitation and temperature generally have opposing influences on glacier mass balance. Observations indicate that warming and increased melting have been the dominant factors compared with accumulation from increased precipitation, with the result that all valley glaciers in the study area are retreating and thinning. Hoodoo Mountain ice cap shows only minor retreat and no evidence of thinning, except that ground-based photography shows restricted thinning at the fringes. Setting aside the climate-insensitive, landform-controlled Hoodoo Mountain ice cap, glaciers spanning a wide range of sizes have similar retreat responses, suggesting that response times for these glaciers are similar and possibly measured around one to a few decades, responding to the past half century (or so) of climate change. If response times were much longer than a few decades, we would not likely see large glaciers responding the same as small ones, and we would not likely see apparent acceleration of glacier responses. If responses were much shorter than a decade, we would see glacier oscillations (not seen in available observations) and asynchronous response behavior. We see two possible explanations: (1) either accelerating glacier changes are tracking accelerating warming and other climatic shifts, or (2) accelerating glacier changes represent a lagged glacier response and increasing gap between actual glacier state and the glacier state needed to keep balance with a steadily warming climate. Possibility #1 would favor a shorter response time, perhaps around a decade, whereas possibility #2 may favor a longer response time, perhaps several decades.

15.3.5.3 *Figure of merit for climate change and energy requirements to drive glacier thinning*

Glacier elevation change rates in our study area during the period from 1965 to ~2005 range from around 0 to −2.7 m/yr, with an average thinning of 0.94 m/yr across the entire glacier area. This rate of thinning is somewhat typical, perhaps a little on the high side of average, for glaciers around the world. To quantify it in energy terms, we do a *gedanken-experiment* (aka thought experiment). Given an ablation area ~60% of the glacier area (a visual estimate), with an assumption that the accumulation areas contribute a net zero value to the thinning rate, the average thinning rate of ablation zones is around 1.57 m/yr. Consider a parcel of a glacier ablation zone that is 1 m^2 in area and initially has a local net annual zero mass balance (i.e., net annual ablation is balanced by ice inflow). How much increase in local energy would be required to turn that parcel of ice into 1.57 m elevation loss each year (due to melting)? Local mass loss is about 1,394 kg/m^2 per year for a glacier density of 890 kg/m^3. For an enthalpy of fusion of ice equal to 334,000 J/kg, an energy flux increase of 466 MJ/m^2 per year is needed to increase melting by the amount correlating to the average thinning rate in the ablation zones of these glaciers. Averaged through the year, this energy increase is 14.8 W/m^2. As melting may be heavily concentrated in just 4 months of the year and ~12 hours per day, the summer daytime energy increase needed is ~89 W/m^2 during the melting period. This compares with the solar constant equal to 1,361 W/m^2, or possibly—just our educated guess—about 550 W/m^2 of direct solar flux during the average period of melting. Thus, the increased melting represented by average thinning in the ablation zones is roughly equivalent to one sixth of guesstimated mean solar flux during melt periods. This may be placed into further context by considering how it compares with insolation changes caused by solar variability of the sunspot cycle; the need for additional energy to cause the high ablation rates is about 80 times the oscillation of solar luminosity due to the sunspot cycle. Thus, the rapid ablation of glaciers in the Hoodoo region, and indeed throughout Canada's coast ranges, clearly mandates a powerful climate change cause.

Obviously, increased melting can be produced by several factors. Increases could be occurring for a number of properties including direct radiant solar flux, sensible heat (average degree-days per summer day, for instance), or length of the melt season. Changes in other environmental variables, such as dust or soot supply, windiness, the seasonality of rainfall could all be involved as well. Decreased ice flow into the ablation zone, such as might occur by reduction in the accumulation zone area or decreased average net annual accumulation rate within that zone, could also contribute to high thinning rates. It is likely that a combination of the above factors could be involved. If due mainly to lengthening of the melt season and not to the warming of summer days, thinning could be explained by half a month increase, from 4 months per year for a balance state to 4.5 months per year, to achieve thinning. Small contributions of each changing variable could sum to cause large average thinning

rates. These are not rigorous glacier accumulation–ablation–climate–ice dynamics modeling calculations; they are rough figures of merit. However, the energy demanded by average thinning represents a large perturbation on the existing glacier system.

15.4 SYNTHESIS AND CONCLUSIONS

These studies add to the variety of methods established that make use of repeat satellite imagery and DEMs for the monitoring of recent and ongoing changes in glaciers. Analysis of remotely sensed data has provided new insights into annual and decadal timescales of changes to glaciers and glacial terrain and highlight the variety of evidence for short-term climatic changes in the Coast Mountains of British Columbia. Rates of terminus retreat of approximately 20–50 m/yr determined from ASTER observations are consistent with ground-based mapping of termini on the century timescale. Thinning rates, however, have accelerated over the past several decades. Mass balance of the glacier area as a whole in the study area has averaged -840 ± 180 kg m^{-2} yr^{-1} from 1965 to 2005, but has increased in magnitude over this period (as the thinning data indicate directly). Details of ice retreat include not only changes in terminus positions and surface elevations, but also extents of ice-marginal lakes and likely vegetation growth on moraines.

Several outlet glaciers in the region analyzed in this study are behaving in much the same way. A 7-year analysis of multispectral image changes, including terminus retreat, and our four-decade-long time series of elevation changes all indicate sustained and primarily accelerating retreat and thinning. The negative balances measured are about the same rate as determined by other researchers for many glaciers in the Canadian Cordillera's Coast Ranges during the past one to several decades. Satellite analysis is supported by a limited set of repeat field imaging over an 11-year period, documenting retreat and thinning of the glaciers and ice caps. Pervasive glacier wastage observed in this area must be a result of climatic forcing, including possibly progressive warming. Presumably other climatic and environmental factors, such as changing wind, cloudiness, and albedo changes related to soot and snow melting, are also involved, but these have not been investigated. Decadal smoothing of available climate records reveals decadal climate oscillations. The response times of all the glaciers appears to be of the order of or longer than a decade, but not more than several decades. Although retreat is not clearly linked to glacier size, thinning rates are variable between glaciers and within individual glacier tongues, and this variability could be related to dynamic differences among the glaciers, as well as to differing microclimates and probably hypsometry. The available evidence suggests that progressive climate change is causing glaciers of all sizes in this area to be increasingly out of balance with their environment, thus driving the acceleration of thinning and retreat.

15.5 ACKNOWLEDGMENTS

J.K. and G.L. thank NASA for support of the GLIMS project, both for imaging by ASTER and a succession of grants that has made our and the consortium activities possible. B.E. thanks the Geological Survey of Canada, NSERC (through operating grants to J.K. Russell), the University of British Columbia, and the Dickinson College Research and Development Committee for generous support of fieldwork at Hoodoo Mountain. We thank the reviewers and also Michael Demuth for helpful tips.

15.6 REFERENCES

Abrams, M., Hook, S., and Ramachandran, B. (1999) *ASTER User Handbook* (NASA document prepared at JPL), NASA Jet Propulsion Laboratory, California Institute of Technology, Pasadena, CA.

Booth, D.B., Troost, K.G., Clague, J.J., and Waitt, R.B. (2003) The cordilleran ice sheet. *Developments in Quaternary Science*, **1**, 17–43, doi: 10.1016/S1571-0866(03)01002-9.

Canadian Daily Climate Data (2007) From Environment Canada. Available at *http://climate.weatheroffice.gc.ca/*

Edwards, B.R. (2010) Hazards associated with alkaline glaciovolcanism at Hoodoo Mountain and Mt. Edziza, western Canada: Comparisons to the 2010 Eyjafjallajokull eruption. *EOS Trans. Am. Geophys. Union*, **87**(52), Fall Meeting Supplement, Abstract NH11B-1132.

Edwards, B.R., and Russell, J.K. (1994) *Preliminary Stratigraphy for the Hoodoo Mountain Volcanic Center, Northwestern British Columbia: Current Research, Part A* (GSC Paper 94-1A), Geological Survey of Canada, Ottawa, Canada, pp. 69–76.

Edwards, B.R., and Russell, J.K. (2002) Glacial influences on morphology and eruptive products of Hoodoo Mountain volcano, Canada. In: J.L. Smellie and M.R. Chapman (Eds.), *Volcano–Ice Interaction on Earth and Mars* (Special Publication 202), Geological Society, London, pp. 179–194.

Edwards, B.R., Edwards, G., and Russell, J.K (1995) *Revised Stratigraphy for the Hoodoo Mountain Volcanic Center, Northwestern British Columbia: Current Research, Part A* (GSC Paper 95-1A), Geological Survey of Canada, Ottawa, Canada, pp. 105–115.

Edwards, B.R., Anderson, R.G., Russell, J.K., Hastings, N.L., and Guo, Y.T. (1999) *Geology of the Quaternary Hoodoo Mountain Volcanic Complex and Adjacent Paleozoic and Mesozoic Basement Rocks; Parts of Hoodoo Mountain (NTS 104B/14) and Craig River (NTS 104B/11) Map Areas, Northwestern British Columbia* (GSC Open File Report, scale 1:20,000), Geological Survey of Canada, Ottawa, Canada.

Edwards, B.R., Russell, J.K., and Anderson, R.G. (2002) Subglacial, phonolitic volcanism at Hoodoo Mountain volcano, northern Canadian Cordillera. *Bulletin of Volcanology*, **64**, 254–272.

Edwards, B.R., Russell, J.K., and Simpson, K. (2010) Volcanology and petrology of Mathews Tuya, northern British Columbia, Canada: Glaciovolcanic constraints on interpretations of the 0.730 Ma Cordilleran paleoclimate. *Bulletin of Volcanology*, doi: 10.1007/s00445-010-0418-z.

Kerr, F.A. (1948) *Lower Stikine and Western Iskut River Areas, British Columbia* (Geological Survey Memoir No. 246), Department of Mines and Resources, [Location], 94 pp.

MacDonald, F.H. (2006) Quaternary geology of Hoodoo Mountain volcano, northwestern British Columbia. Unpublished M.Sc. thesis, University of Calgary, 138 pp.

Martínez-Alonso, S., Mellon, M.T., Banks, M.E., Keszthelyi, L.P., McEwen, A.S., and the HiRISE Team (2011) Evidence of volcanic and glacial activity in Chryse and Acidalia Planitiae, Mars. *Icarus*, **212**, 597–621, doi: 10.1016/j.icarus.2011.01.004.

Russell, J.K., Stasiuk, M.V., Page, T., Nicholls, J., Rust, A., Cross, G., Schmok, J., Edwards, B.R., Hickson, C.J., and Maxwell, M. (1998) *The Ice Cap of Hoodoo Mountain Volcano, Northwestern British Columbia: Estimates of Shape and Thickness from Surface Radar Surveys: Current Research, Part A* (GSC Paper 98-1A), Geological Survey of Canada, Ottawa, Canada, pp. 55–63.

Ryder, J.M., and Maynard, D. (1991) The Cordilleran ice sheet in northern British Columbia. *Géographie physique et Quaternaire*, **45**(3), 355–363.

Schiefer, E., Menounos, B., and Wheate, R. (2007) Recent volume loss of British Columbian glaciers. *Geophysical Research Letters*, **34**, L16503, doi: 10.1029/2007GL030780.

Shea, J.M., Menounos, B., Moore, R.D., and Tennant, C. (2012) Regional estimates of glacier mass change from MODIS-derived equilibrium line altitudes. *The Cryosphere Discussions*, **6**, 3757–3780, *www.the-cryosphere-discuss.net/6/3757/2012/*, doi: 10.5194/tcd-6-3757-2012.

Smellie, J.L. (2009) Terrestrial sub-ice volcanism: Landform morphology, sequence characteristics and environmental influences, and implications for candidate Mars examples. In: M.G. Chapman and L. Leszthely (Eds.), *Preservation of Random Mega-scale Events on Mars and Earth: Influence on Geologic History* (GSA Special Paper No. 453), Geological Society of America, Boulder, CO, pp. 55–76.